Mapping the sequences of potential guanine quadruplex motifs

Alan K. Todd and Stephen Neidle*

CRUK Biomolecular Structure Group, The School of Pharmacy, University of London, 29-39 Brunswick Square, London WC1N 1AX, UK

ABSTRACT

The knowledge that potential guanine quadruplex sequences (PQs) are non-randomly distributed in relation to genomic features is now well established. However, this is for a general potential quadruplex motif which is characterized by short runs of guanine separated by loop regions, regardless of the nature of the loop sequence. There have been no studies to date which map the distribution of PQs in terms of primary sequence or which categorize PQs. To this end, we have generated clusters of PQ sequence groups of various sizes and various degrees of similarity for the non-template strand of introns in the human genome. We started with 86 697 sequences, and successively merged them into groups based on sequence similarity, carrying out 66 clustering cycles before convergence. We have demonstrated here that by using complete linkage hierarchical agglomerative clustering such PQ sequence categorization can be achieved. Our results give an insight into sequence diversity and categories of PQ sequences which occur in human intronic regions. We also highlight a number of clusters for which interesting relationships among their members were immediately evident and other clusters whose members seem unrelated, illustrating, we believe, a distinct role for different sequence types.

INTRODUCTION

The occurrence of potential guanine quadruplex sequence motifs (PQs) within non-telomeric nucleic acids has been the subject of a number of studies (1–14) (for reviews, see refs 15 and 16) and several databases and web resources are available (17–21). Most of the emphasis of these surveys has been to examine the number of PQs and the genomic regions in which they occur. Several studies of individual and specific sequences at a small number of loci have been carried out. In particular, PQs associated with the promoter regions of the *c-kit* (22–25) and *c-myc* (26,27) genes have been examined in detail, as well as the 5′-untranslated region (UTR) region in several other genes including N-ras (28) and zic-1 (29). Apart from our initial analysis describing loop sequences within PQ sequences (1), there has been no systematic classification of PQs in terms of their primary sequence. Crystallographic, nuclear magnetic resonance (NMR) and modelling studies have demonstrated that the topology of guanine quadruplexes is very dependent on their primary sequence, as found, for example, in various human telomeric sequences (30–33), and the two *c-kit* sequences (22–25). Biophysical studies of loop size (34–36) and analyses of the effects of sequence in single-base loops (37) also confirm this conclusion.

From the outset of sequence-based studies into potential quadruplex sequences in non-telomeric nucleic acids, it has been clear that there are more sequences than can be experimentally studied, and to date only a very small fraction of the individual sequences have been examined, although there have been attempts to establish some more general rules governing the energetics of quadruplexes (38). Our initial survey of PQs in the human genome showed that there are 226 157 unique sequences that concur with our search criterion (1). In the same study, we carried out a detailed examination of loop sequences and established that in terms of sequence space, the distribution of loop sequences is far from random, with some being very common and many others not appearing at all. However, examining loop sequences in this way is problematic since, in instances with variable numbers of guanines in the G-tracts and/or isolated guanines in loop sequences, it is not currently possible to determine which guanines are part of the loop and which are part of the G-quartet core, in the absence of relevant experimental data. When more than four G-tracts are present in a sequence, we have the additional problem of determining which of them would participate in a more stable quadruplex structure. We thus need a more practical

*To whom correspondence should be addressed. Tel: +44 207 753 5969; Fax: +44 207 753 5970; Email: stephen.neidle@pharmacy.ac.uk

and robust way of studying quadruplex sequences in detail than trying to derive information from loop sequences alone. In this study, we consider the sequences of potential quadruplex-forming regions as a whole rather than their component parts (G-tracts and loop regions) and describe a method for finding groups of similar sequence. This removes any need to make prior assumptions about topology. Finding many examples of a complex sequence is compelling evidence of positive selection. The possibility therefore exists that quadruplex structure is the reason for such selections. Of the clusters which contain sequence that are proven to form G-quadruplex structures, there is also the possibility that similar sequences may also form similar folding topologies. We have used the non-template strand of introns in the human genome to develop our method and at the same time to produce new data on quadruplex sequences within introns. Our goals are therefore to develop a method to find groups of similar short sequence, apply it to potential guanine quadruplex sequences and, subsequently, determine whether one can find correlations within these groups or something to link the genes in which the sequences occur. In addition, the application of this method can be seen as a hypothesis-generating exercise, as the potential guanine quadruplex clusters can be used as a starting point for further analyses. We have therefore chosen a number of clusters to illustrate that different types of correlation can be found in the clusters.

Hierarchical agglomerative clustering is a method with which one starts with the individual data and merges the most similar (39). The resulting clusters are then successively merged until only one cluster remains. One ends up with a grouping of data in a dendrogram where, at successive levels, the cluster members are less similar. This is schematically represented in Figure 1. In order to cluster nucleic acid sequences in such a way, a similarity metric is needed, and for this, pair-wise sequence alignments were carried out and a similarity score was obtained. Once a similarity metric has been established, there are a number of ways to compare clusters. In this instance, the complete linkage method has been used, where the distance between two clusters is the score of the least-similar, longest distance between any member of one cluster to any member of the other.

METHODS

All genomic data were taken from the ENSEMBL database (40) homo_sapiens_core_57_37b and the non-template strand sequences were extracted from the intronic regions for all genes with status 'known'. The same method was used in earlier studies (1,5) to gather the G-rich sequences with the pattern: $G_{3-5}L_{1-7}G_{3-5}L_{1-7}G_{3-5}L_{1-7}G_{3-5}$, where G represents guanine bases and L represents any base including guanine. The ENSEMBL perl API was used to extract the genomic regions of interest and in-house software written in C++ used to extract the PQ regions. Regions that had more than four G-tracts were treated as a single sequence. A total of 101 926 potential quadruplex-forming regions
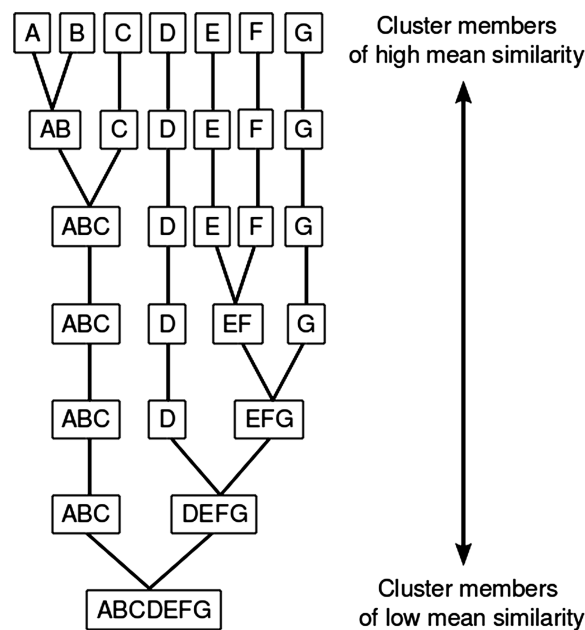

Figure 1. The clustering process begins at the top, where the individual data are treated as clusters. The most similar data are merged, the similarity between the new clusters is derived and the most similar of those are merged until all of the data are in the same cluster.

were extracted; however, a number of identical sequences were identified in this set, giving 86 697 unique sequences. The sequences were then collated into a mySQL database, along with information about their genomic locations.

Sequence alignments and clustering were carried out using in-house software written in C++. The Smith–Waterman method was used as described by Durbin *et al.* (41) to carry out the individual alignments. The scoring scheme is quite simple since all mismatches are considered equal. Match = 1, mismatch = 0, gap = −0.5 edge-gap = 0. Edge-gaps are the over-hanging part at the end of the sequences which arise from the fact that the sequences are often of different lengths, so edge-gaps are inevitable and therefore less costly than gaps within the sequence.

The scoring for the clustering was carried out in a different way from that of the pair-wise sequence alignments, since there is a different purpose for each of these. It was done by counting the number of gaps and mismatches dividing by the number of potential matches. The maximum number of matches in any alignment is the length of the shortest sequence. Since gaps in the longer sequence lead to fewer matches, we only penalize gaps on the shorter sequence.

The scoring scheme used is described in the following. Details of this scheme and our rationale behind it can be found in the Supplementary Data. To avoid confusion these are not being called 'alignment scores' because they were not obtained when the alignments were carried out, but rather they are 'similarity scores'. This now provides a metric of sequence similarity which is independent of the lengths of the sequences involved.

We also obtained more clear-cut results for the clustering by separating the two scoring schemes. The pair-wise sequence alignments were done to find the 'best' alignment between the sequences, and the scores for the clustering were calculated so that one pair-wise sequence alignment can be compared with another. It was necessary to score them independently of size since the pair-wise alignments can be of varying size. (Supplementary Figure S1 and Table S4 illustrate how the clustering was biased towards longer sequences being clustered first when using the alignment scores for the clustering from a subset of 1000 sequences chosen at random.)

The scoring scheme that we developed was effectively our definition of sequence similarity and had to compare alignments of various lengths. There are many ways in which we could score our alignments, depending on how we define sequence similarity, which would possibly produce differing results, e.g. scoring mismatches higher than gaps might be sensible if we decided that guanine quadruplex loop length was more important to stability than base composition. However, we wish to assume as little as possible and so have kept the scoring scheme as simple as we can. We believe that the results from the method that we settled on indicates that it fits the purpose well.

To compare whole clusters, full-linkage hierarchical agglomerative clustering was used. When attempting to use single-linkage and mean linkage hierarchical agglomerative clustering, it was found that the clusters were subject to an unacceptable amount of chaining, where unrelated sequences can end up belonging to the same cluster. This method was very computer-intensive since to measure the similarity score between two clusters, every pair of sequences between the two clusters must be aligned. The similarity matrix was too large to be held in computer memory (~28 Gb of data). It was found that it was faster to pre-compute all of the sequence alignments (3 758 141 556 alignments), calculate the comparison scores and store them on a hard drive, since looking up the scores from the hard drive was faster than carrying out the alignment and obtaining the similarity scores on the fly.

The clustering process went as follows:

(i) Set similarity threshold to 1 and consider each sequence as a cluster.
(ii) Compare all clusters and when a pair is found which has a score equal to or better than the similarity threshold, merge them together.
(iii) Repeat stage 2 until there are no longer any pairs of clusters at or above the similarity threshold.
(iv) Decrease the similarity threshold by 0.05 and go back to stage 2.

The process at stage 2 is traditionally performed by merging the best pair of clusters and re-calculating the similarity scores between the newly formed cluster and the remaining clusters. However, this would have taken an impossibly long time with such a large number of sequences, since cluster comparisons are very costly in terms of computer time. To expedite the process, a coarse-grained approach was adopted which merged many of the clusters in a single cycle and greatly reduced the number of cluster comparisons that were carried out. By decreasing the similarity threshold by 0.05 increments every time, the process was greatly speeded up; we suggest that the outcome was not significantly different from what would have happened if it were practical to cluster by re-calculating the score matrix after every merging. (A comparison of the performance of both methods can be found in Supplementary Figure S2.) The clusters formed at the last cycle before the similarity threshold was dropped, thereby being of most interest. The degree of similarity of the cluster members can be derived from the similarity threshold and hence is related to the cycle number. The earlier in the clustering, the more similar are the cluster members.

Several prominent clusters were chosen and dendrograms drawn with software that was developed in-house, using the Python Imaging Library and the *aggdraw* module, in the Python programming language. We also carried out multiple sequence alignments between the cluster members for the purposes of illustration using ClustalW (42).

We used FuncAssociate 2.0 (43) which employs the Fisher's exact test to determine the probability that gene ontology (44) (GO) terms are over-represented [the null hypothesis is that it is unsurprising that the number of any particular GO term appears in the test set (Cluster) by chance]. Since it is not impossible to find false positives when looking for correlations in large sets of data, FuncAssociate calculates an adjusted *P*-value that includes an estimation of the probability of obtaining at least one false positive. The list of genes belonging to each of the clusters produced by Cycles 5, 9, 13, 17, 20, 23, 26, 29, 32, 36, 39, 42, 45 and 48 whose sequences were associated with more than 10 different genes were sent to the FuncAssociate server. A *P*-value cut-off of 0.05 was used to determine which clusters were over-represented in any GO term.

RESULTS

Cluster size distribution

Figure 2 shows how the number of clusters decreases at each cycle. The threshold level is also shown and it can be seen at which cycles the similarity threshold was decreased and how this affects the number of clusters. For example, between Cycles 7 and 8 the largest drop in the number of clusters occurs, from 72 106 to 56 049 clusters. The next significant drop, between Cycles 11 and 12 (55 802–39 852 clusters), is almost as large. These are, therefore, the stages with the largest number of clusters merging and coincide with the similarity threshold decreasing from 0.95 to 0.9 and from 0.9 to 0.85.

Figure 3 shows the cluster size distribution changing with each cluster cycle, for clusters containing between 1 and 400 sequences and on the final column for clusters larger than 400. The clusters were arranged in bins depending on the number of sequence members which they contained, starting with clusters with 0–10 members, then
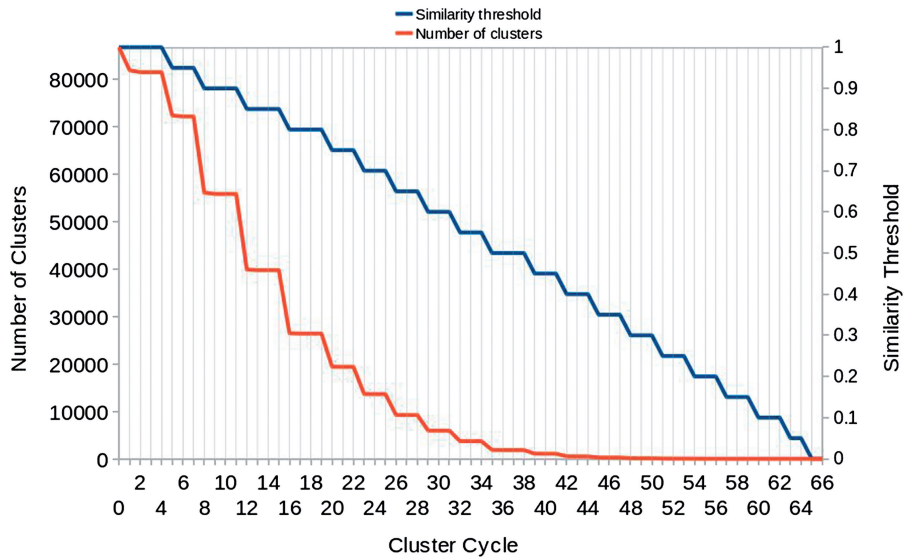
Figure 2. The relationship between the similarity threshold and the number of clusters during the progression of the clustering process.
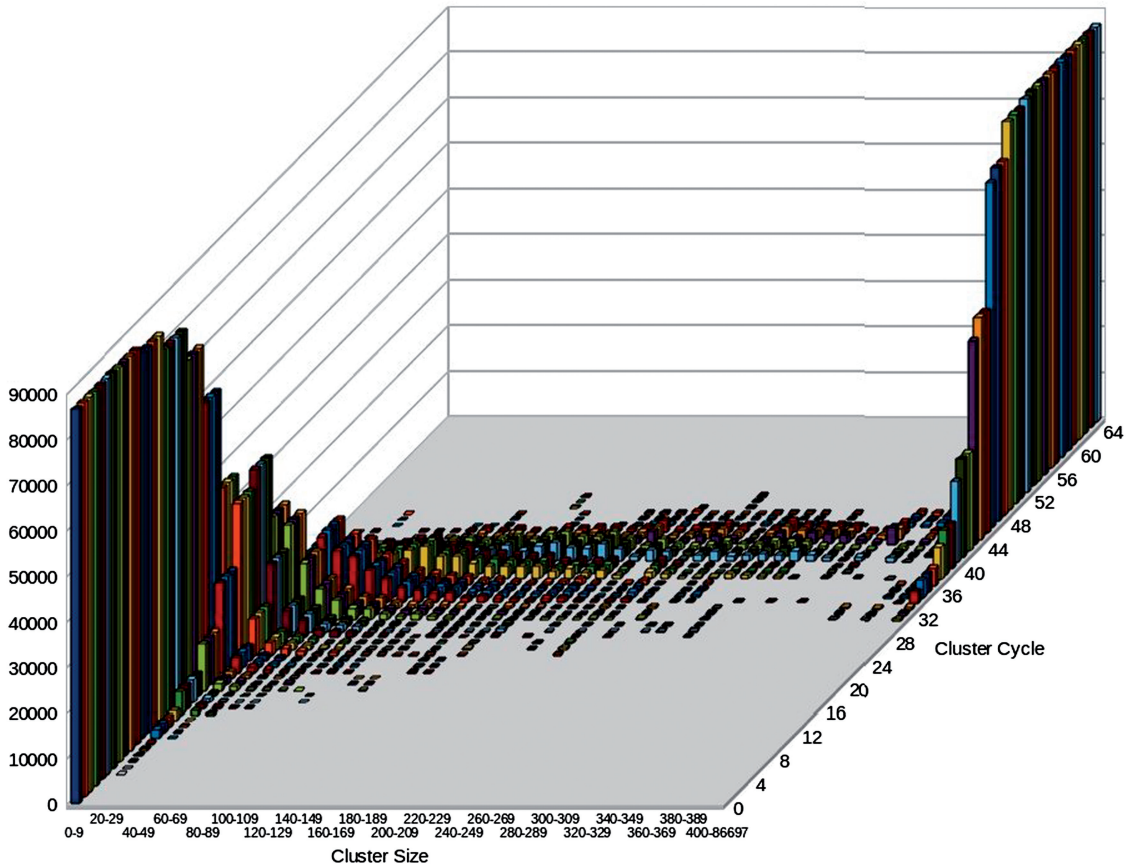

Figure 3. The distribution of cluster members by cluster size and the progression of the clustering process.

10–20 members and so on until the clusters along the right-hand side with 400–86 696 sequence members. The heights represent the total number of sequences within the clusters in a particular bin and each coloured row represents a cluster cycle. It can be seen that, as expected, the sequences are initially distributed among the small clusters

(0–10) and it is not until Cycle 5 that there are clusters with greater than 10 sequences in them. By Cycle 27 the number of clusters containing 0–10 sequences is dropping significantly and the sequences are distributed among larger clusters and by Cycle 31 there are clusters which contain more than 400 sequences. As the process of

merging clusters continues, the distribution moves to the right until by Cycle 56 there are no longer any clusters below 400 sequences and finally at Cycle 65 the clustering has converged into a single cluster.

There are a very large number of clusters and to carry out a detailed manual analysis of all of them would be unfeasible. We have therefore taken several clusters and highlighted some interesting features within them. Diagrams of these clusters show the multiple sequence alignments calculated using the program ClustalW next to the dendrograms generated from the clustering data. Many of the groupings in the dendrogram on the right can be correlated to features of the ClustalW-aligned sequences even though they were derived through different means. For example, in Figure 5a sequences 8–10, which share very similar sequences over the first 17 bases, are grouped together much earlier in the clustering process than they are with the rest of the sequences in the cluster which differ in this region.

Figure 4 and Table 1 show Cycle 27 cluster number 4470, which contains a cluster of human telomere and human telomere-like sequences with the potential to form quadruplex structures. Azzalin *et al.* (45) and Schoeftner and Blasco (46) showed that telomeres are not transcriptionally silent and that the C-rich strand is transcribed more than the G-rich strand, resulting in r(UUAGGG)$_n$ being more abundant than r(CCCUAA)$_n$. These G-rich RNAs can interact with telomeric DNA and also with the telomerase RNA template and thus inhibit the catalytic action of the telomerase enzyme complex. They can also interact with other gene products such as that of SMG which are also involved in the maintenance of telomeres. The clusters that we have here are examples of an area where this new class of RNA could also be transcribed. Although these sequences are within introns, it is not inconceivable that they can exist alone or as part of smaller molecules after splicing and digestion. For example, it was been observed (47) that while in the quadruplex form, G-rich telomeric RNA is immune to digestion by T1 nuclease, which normally cleaves RNA after a single-stranded guanine residue. Further detail on these clusters is given in Supplementary Tables 1S and 2S. Locating telomeric

repeats in non-telomeric DNA has been previously observed, albeit not at the sequence level—for example Meyne *et al.* (48) discussed their distribution in 100 vertebrate species.

Figure 5a and b and Tables 2 and 3 show clusters which are mainly composed of closely related zinc-finger genes. The members of the cluster in Figure 5a all belong to the same *interpro* (49) families, IPR001909 Krueppel-associated box and IPR007087 Znf_C2H2. They occur at 13 different locations, with 10 unique sequences. The location of the sequences within the genes is similar for most of these genes, usually about 200–300 bases from the beginning of the first intron. The variable parts of the sequence tend to be outer 'loops' while the central GGG AGGG core appears to be conserved. This is also conserved in another very similar cluster shown in Figure 5b. The majority of those genes belong to the same *interpro* families, IPR001909 Krueppel-associated box and IPR007087 Znf_C2H2. Sequence 7 is shared by two genes which overlap, AC010300.1 and ZNF91. ZNF91 being contained entirely within an intron of AC010300.1. Almost all of these genes are found in the same area of chromosome 19; however, two genes are found in entirely different locations, ZNF107 is found on chromosome 7 and MAP1B is found on chromosome 5. Although MAP1B is an unrelated gene, its expression has been shown to be controlled by the zinc finger gene BCL11A which also belongs to *interpro* family IPR007087 Znf_C2H2 (50). When looking at the variable and conserved regions, we need to be aware that the search criterion may have an effect on what we see, i.e. be cognizant of the fact that we will always have conserved runs of guanines in the sequences. It may be more instructive to look at the conservation of the loop sequences; however, if the guanine runs are longer than three bases, there is scope for variability around the edges, under our search criterion. The cluster in Figure 5a appears to be more variable in the region of the first loop while the central 'A' loop is the same throughout and the third loop 'TCAT' has only one difference, a substitution of an adenine for a cytosine. Since the final G-runs are longer than three bases, we see two cases where the guanines are substituted for an adenine and for a thymine.
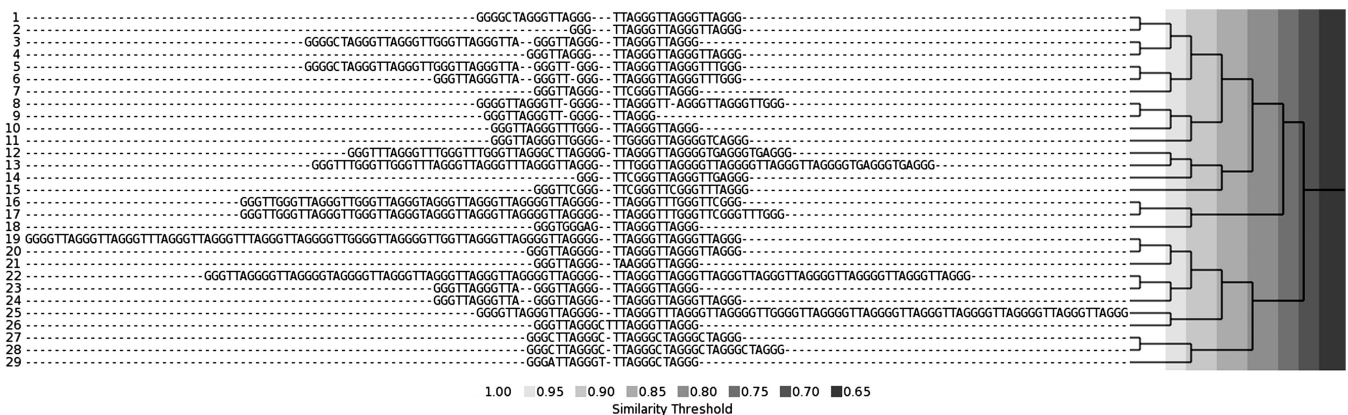

Figure 4. Telomeric like quadruplex sequences.

Table 1. Telomeric sequence clusters

Leaf no.	Gene	EnsemblID	From start	To end	Feature
1	BET1L	ENSG00000177951	4603	6519	Intron 4–5
2	ST8SIA1	ENSG00000111728	7933	39 013	Intron 4–5
	MRVI1	ENSG00000072952	28 383	31 060	Intron 1–2
3	BET1L	ENSG00000177951	4408	6697	Intron 4–5
4	EHD4	ENSG00000103966	2730	7842	Intron 2–3
	ARNT2	ENSG00000172379	5495	6719	Intron 3–4
	ARFGAP3	ENSG00000242247	5564	18 179	Intron 1–2
5	BET1L	ENSG00000177951	4512	6588	Intron 4–5
	BET1L	ENSG00000177951	4713	6387	Intron 4–5
6	BET1L	ENSG00000177951	4839	6279	Intron 4–5
7	NLGN4X	ENSG00000146938	39 962	81 579	Intron 2–3
8	CBFA2T3	ENSG00000129993	458	762	Intron 8–9
9	RP11-40F6.1	ENSG00000237523	8711	1055	Intron 1–2
10	RP11-416N4.2	ENSG00000230506	17 796	5299	Intron 1–2
11	AC004490.2	ENSG00000234432	18 343	8360	Intron 1–2
12	BET1L	ENSG00000177951	3916	7179	Intron 4–5
13	FAM157C	ENSG00000233013	5783	6648	Intron 3–4
14	ZNF275	ENSG00000063587	329	846	Intron 3–4
15	BET1L	ENSG00000177951	3830	7298	Intron 4–5
16	BET1L	ENSG00000177951	3753	7335	Intron 4–5
17	FAM157C	ENSG00000233013	5638	6804	Intron 3–4
18	CALN1	ENSG00000183166	26 860	7885	Intron 1–2
19	RPL23AP82	ENSG00000184319	967	2391	Intron 3–4
	RPL23AP7	ENSG00000226019	967	2391	Intron 2–3
20	RP11-218L14.1	ENSG00000225393	8722	9458	Intron 1–2
21	ARHGEF3	ENSG00000163947	9469	66 708	Intron 2–3
22	BET1L	ENSG00000177951	13 701	11 400	Intron 3–4
23	KCNJ6	ENSG00000157542	4819	120 673	Intron 2–3
	RP1-207H1.1	ENSG00000231150	8043	8579	Intron 1–2
24	CFDP1	ENSG00000153774	60 850	29 018	Intron 5–6
25	AL078621.1	ENSG00000228003	969	12 303	Intron 1–2
26	AC068541.3	ENSG00000233897	51 142	108 760	Intron 3–4
27	BET1L	ENSG00000177951	3715	7412	Intron 4–5
28	FAM157C	ENSG00000233013	5594	6887	Intron 3–4
29	SLC8A2	ENSG00000118160	2410	762	Intron 6–7

Within Cycle 18, several clusters were found to be over-represented in the GO term GO:0003823 'antigen binding'. Cycle 18 cluster 13 461 (Figure 6 and Table 4) is one such cluster, which consists mainly of LIR genes (leucocyte immunoglobulin-like receptor). These genes are all found in the same genomic location: region 19q13.4. All but one of the genes in the cluster occur at this location; however, since some of the genes are overlapping, the total number of locations is 11. Cycle 18 cluster 448 (Figure 7 and Table 5) contains a number of sequences which occur within two immunoglobulin genes, IGHA2 and IGHM which contain a number of very similar sequences. A third IGH gene IGHV3-6 is a pseudogene; however, since certain pseudogenes may play an important role in regulation (51,52), this may still be a biologically relevant locus. Three other genes which appear in this cluster, TRIM29, ZNF831 and BRSK2, are unrelated to the immunoglobulins. A similar cluster, Cycle 18 cluster 1086, (Figure 8 and Table 6), contains the same immunoglobulin genes and similar sequence motifs. This also contains three non-immunoglobulin genes KCNK2, SMAD and the same kinase gene as found in the aforementioned cluster, BRSK2. Closer examination of the regions in which these sequences occur in both the immunoglobulin genes and the BRSK2 suggests that they
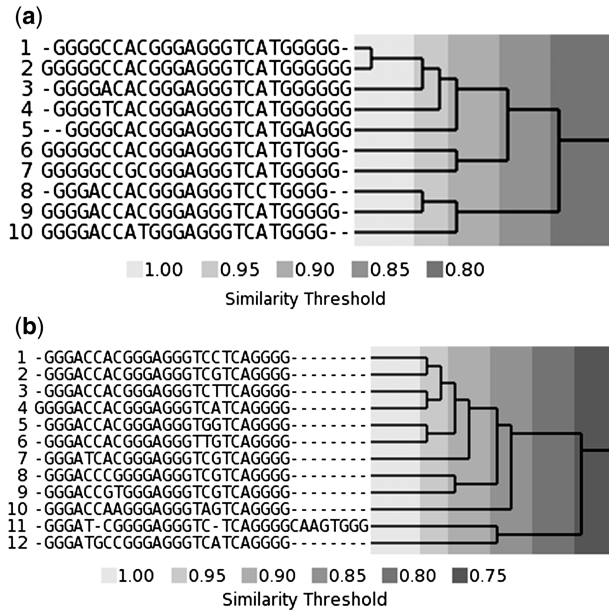

Figure 5. (**a**) Cycle 18 cluster 202 zinc finger type genes 1. (**b**) Cycle 21 cluster number 4672 zinc finger genes.

Table 2. Cycle 18 cluster 202 zinc finger type genes 1

Leaf no.	Gene	EnsemblID	From start	To end	Feature
1	ZNF844	ENSG00000223547	300	8830	Intron 1–2
2	ZNF491	ENSG00000177599	289	5499	Intron 1–2
3	ZNF833	ENSG00000197332	286	4031	Intron 1–2
4	ZNF709	ENSG00000242852	247	46 621	Intron 1–2
	ZNF564	ENSG00000196826	37 833	46 621	Intron 1–2
5	ZNF709	ENSG00000242852	29 380	17 489	Intron 1–2
	ZNF564	ENSG00000196826	66 966	17 489	Intron 1–2
6	ZNF69	ENSG00000198429	279	15 324	Intron 1–2
7	ZNF627	ENSG00000198551	228	16 643	Intron 1–2
8	ZNF791	ENSG00000173875	211	12 383	Intron 1–2
9	ZNF20	ENSG00000132010	290	3960	Intron 1–2
	ZNF625	ENSG00000213297	290	3960	Intron 5–6
10	ZNF44	ENSG00000197857	6496	15 598	Intron 4–5

Table 3. Cycle 21 cluster number 4672 zinc finger genes

Leaf no.	Gene	EnsemblID	From start	To end	Feature
1	AC011477.1	ENSG00000245381	31 177	25 473	Intron 2–3
2	ZNF100	ENSG00000197020	279	1336	Intron 1–2
	ZNF681	ENSG00000196172	264	2906	Intron 1–2
3	ZNF431	ENSG00000196705	288	1051	Intron 1–2
4	ZNF493	ENSG00000196268	286	7549	Intron 1–2
5	ZNF492	ENSG00000229676	290	18 517	Intron 1–2
6	ZNF85	ENSG00000105750	282	10 313	Intron 1–2
7	AC010300.1	ENSG00000235694	71 073	70 836	Intron 9–10
	ZNF91	ENSG00000167232	287	20 248	Intron 1–2
8	ZNF254	ENSG00000213096	272	18 305	Intron 1–2
9	ZNF738	ENSG00000172687	289	2308	Intron 1–2
10	ZNF724P	ENSG00000196081	287	17 634	Intron 1–2
11	MAP1B	ENSG00000131711	41 788	26 124	Intron 2–3
12	ZNF588	ENSG00000196247	322	12 544	Intron 1–2

are all part of a larger region of similarity. That we have closely related genes with similar sequences within their introns is perhaps no great surprise; however, the existence of similar sequences within the introns of unrelated genes is an unexpected observation.

Cycle 18 cluster 2 (Figure 9 and Table 7) contains 27 sequences; however, many occur in more than one locus and the sequences in the cluster appear 140 times. Sequences 1 and 5 are the most common, occurring 45 and 51 times, respectively. We used biomart (53) in the ENSEMBL website to retrieve the *interpro* (49) IDs for the genes involved (full details are given in the Supplementary Data). Of the 88 genes which had *interpro* mappings, several were related; however, none occurred more than seven times and the genes are distributed over a range of gene families. Among them
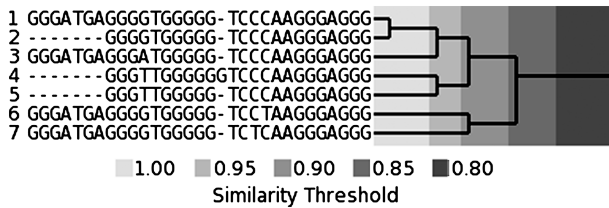
are kinases, zinc-finger genes, RAB/RAS genes, WD-40 domains and catenins. Many are known to be associated with signal-transduction pathways (RIN3, TBC1D19, RASGRF3, CDK14, ARHGAP6, CTNNA3 and CTNND2, to name a few) and many are involved in mitosis (CENPQ, PARD3B, ALMS1, SPTLC1, etc.). This cluster demonstrates a significant number of genes both related and unrelated, which contain similar and often identical PQ sequences.

Using the FuncAssociate tool to characterize gene sets, we discovered that a number of clusters were over-represented in certain GO terms. The results are summarized in Table 8, which shows, for each cycle, the number of clusters whose sequences fell in more than 10 ENSEMBL genes, the number of these which were over-represented in GO terms, the sum of the number of GO terms which were found to be over-represented in each cluster and the percentage of chosen clusters in which were found to be over-represented in GO terms. The percentage of clusters examined which contained over-

Figure 6. Cycle 18 cluster 1346. Cluster containing sequences that occur chiefly within leukocyte immunoglobulin-like receptor (LIR) genes.

Table 4. Cycle 18 cluster 13 461. Cluster containing sequence which occur chiefly within leucocyte immunoglobulin-like receptor (LIR) genes

Leaf no.	Gene	EnsemblID	From start	To end	Feature
1	LILRA6	ENSG00000244482	77	147	Intron 5–6
	LILRB3	ENSG00000204577	77	147	Intron 5–6
	LILRB3	ENSG00000204577	18 899	1733	Intron 7–8
2	LILRA1	ENSG00000104974	617	3193	Intron 5–6
	LILRB1	ENSG00000104972	21 906	35 443	Intron 2–3
	LILRP2	ENSG00000240258	84	146	Intron 3–4
	AC006293.1	ENSG00000170858	84	146	Intron 4–5
3	LILRB1	ENSG00000104972	77	148	Intron 5–6
4	KCNH2	ENSG00000055118	446	30	Intron 8–9
5	LILRA2	ENSG00000239998	84	147	Intron 6–7
	LILRB1	ENSG00000104972	1525	55 824	Intron 2–3
6	LILRA4	ENSG00000239961	79	147	Intron 5–6
	LILRA3	ENSG00000170866	77	146	Intron 9–10
7	AC011515.1	ENSG00000225370	77	153	Intron 2–3

Table 5. Cycle 18 cluster 448. Cluster containing sequences which occur in immunoglobulin genes IGHA2 and IGHM

| Leaf no.	Gene	EnsemblID	From start	To end	Feature
1	IGHA2	ENSG00000211890	1459	1736	Intron 1–2
2	TRIM29	ENSG00000137699	8326	383	Intron 1–2
3	IGHA2	ENSG00000211890	979	2231	Intron 1–2
4	IGHA2	ENSG00000211890	472	2763	Intron 1–2
5	IGHA2	ENSG00000211890	844	2321	Intron 1–2
6	IGHA2	ENSG00000211890	549	2701	Intron 1–2
7	IGHA2	ENSG00000211890	1084	2106	Intron 1–2
8	IGHA2	ENSG00000211890	1749	1486	Intron 1–2
9	IGHV3-6	ENSG00000233855	5773	86 881	Intron 10–11
	IGHM	ENSG00000211899	2872	2301	Intron 1–2
10	IGHV3-6	ENSG00000233855	3982	88 648	Intron 10–11
	IGHM	ENSG00000211899	1081	4068	Intron 1–2
11	BRSK2	ENSG00000174672	517	3328	Intron 12–13
12	IGHV3-6	ENSG00000233855	5943	86 716	Intron 10–11
	IGHV3-6	ENSG00000233855	5983	86 676	Intron 10–11
	IGHM	ENSG00000211899	3042	2136	Intron 1–2
	IGHM	ENSG00000211899	3082	2096	Intron 1–2
13	ZNF831	ENSG00000124203	15 164	30 732	Intron 3–4
14	IGHV3-6	ENSG00000233855	4833	87 826	Intron 10–11
	IGHV3-6	ENSG00000233855	4884	87 775	Intron 10–11
	IGHV3-6	ENSG00000233855	5274	87 385	Intron 10–11
	IGHM	ENSG00000211899	1932	3246	Intron 1–2
	IGHM	ENSG00000211899	1983	3195	Intron 1–2
	IGHM	ENSG00000211899	2373	2805	Intron 1–2
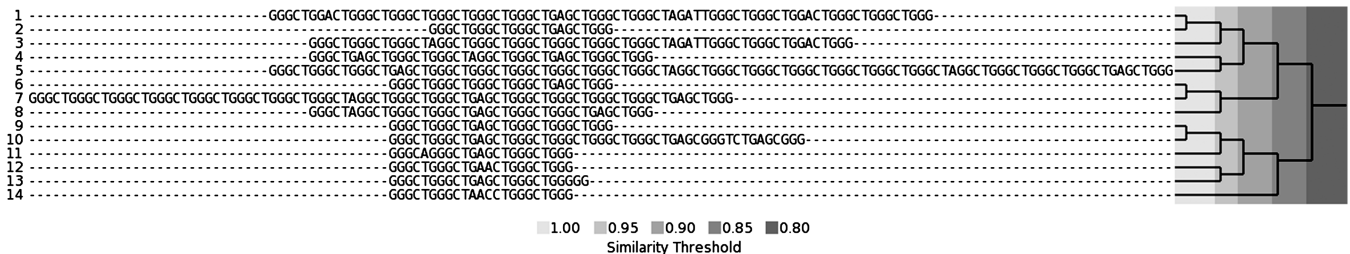
Figure 7. Cycle 18 cluster 448. Cluster containing sequences that occur chiefly in immunoglobulin genes IGHA2 and IGHM.
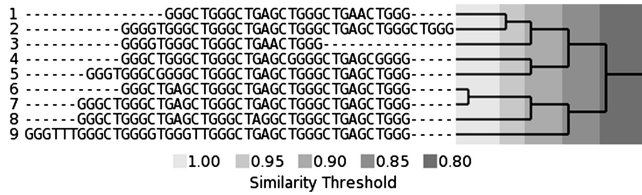
Figure 8. Cycle 18 cluster 1086. Cluster containing sequences that occur chiefly in immunoglobulin genes IGHA2 and IGHM.

Table 6. Cycle 18 cluster 1086. Cluster containing sequences which occur chiefly in immunoglobulin genes IGHA2 and IGHM

| Leaf no.	Gene	EnsemblID	From start	To end	Feature
1	IGHV3-6	ENSG00000233855	6237	86 417	Intron 10–11
	IGHM	ENSG00000211899	3336	1837	Intron 1–2
2	IGHA2	ENSG00000211890	2392	848	Intron 1–2
3	KCNK2	ENSG00000082482	61 113	19 276	Intron 1–2
4	IGHV3-6	ENSG00000233855	4247	88 402	Intron 10–11
	IGHM	ENSG00000211899	1346	3822	Intron 1–2
5	BRSK2	ENSG00000174672	363	3468	Intron 12–13
6	IGHA2	ENSG00000211890	1654	1591	Intron 1–2
7	IGHV3-6	ENSG00000233855	4052	88 592	Intron 10–11
	IGHM	ENSG00000211899	1151	4012	Intron 1–2
8	IGHV3-6	ENSG00000233855	4197	88 447	Intron 10–11
	IGHM	ENSG00000211899	1296	3867	Intron 1–2
9	SMAD1	ENSG00000170365	10 591	14 155	Intron 2–3
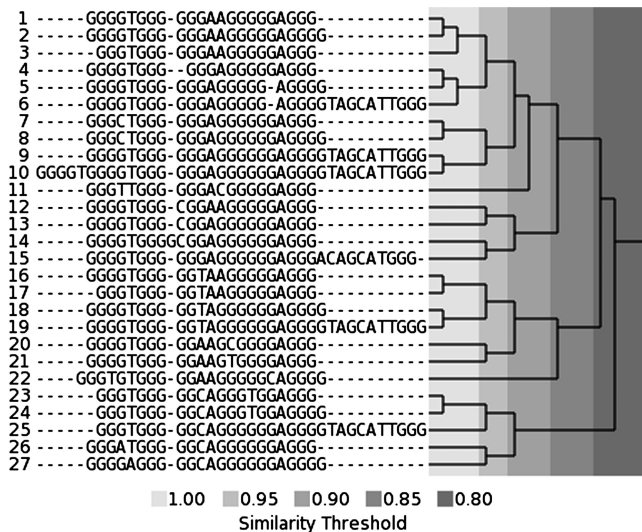
Figure 9. Cycle 18 cluster 2. This shows sequences that occur in unrelated genes.

represented GO terms did not vary dramatically for clusters 5–39 where it began at 12% for Cycle 5 and remained for the most part between 9% and 10%. At cluster 49 it began to rise, 18% for Cycle 49, 24% for Cycle 45 and 48% for Cycle 48. This approximately steady rate at Cycles 5–39 is probably due to the fact that while new clusters are being formed and genes

Table 7. Cycle 18 cluster 2. Sequences which occur in unrelated genes. List of genes in which each sequence in this cluster occurs

1 **CHST9** CTNND2 **PDZD2** TBC1D19 **PDE4D** TRIM5 **PLCB1** LRRC9 **TMEM170B** AP000705.4 **LRRK2** SUMF1 **NELL1** MEGF10 **FBN2** AP003355.2 **VPS13B** AC090922.1 **AC096733.1** RNF150 **WDFY4** ALK **SLC16A7** GLIPR1L2 **SEMA3D** EIF4G3 **PFTK1** C2orf34 **DLG2** F8 **RP11-451L9.1** FRMD4B **ZNF28** ZNF665 **PDE4B** AC010132.1 **CTB-111H14.1** AC009264.1 **COL24A1** RP11-457K10.1 **DYTN** KCNE4 **AC007254.1** RAB3GAP2 **RP11-479J7.2**
2 RIN3
3 PTPRD
4 **NBEA** FBXL5 **KLF12** ADAMTS3 **SLC24A3** RASGRF2 **BICD1** BEND7 **AP000235.2** LACTB2 **FAM190A** C11orf74 **TBCK** AMBRA1 **PSMC1** TEX11 **PPP2R2B** KIAA2022 **SPTLC1** MAGT1 **CTNNA3** ODZ3 **UQCRFS1** AC008413.1 **MON2** C11orf80 **CENPQ** NRCAM **TRIM77** AC003050.1 **ATRNL1** FXYD6 **RP11-702L6.4** SLC9A10 **STXBP5L** RP11-310E22.1 **CASC2** AC005582.1 **ST6GALNAC3** RP4-630C24.1 **LRP1B** GALNT13 **SLC25A24** RP11-439L18.3 **AC018359.2** PTH2R **AC079613.1** AC093865.2 **RP11-542C10.1** RP11-202K23.1 **RP11-479J7.2**
5 RP11-735B13.1
6 PK4P
7 DLG2
8 PTPRD
9 AF127577.3 **AGBL1** AFF2 **CYP4B1** AC003090.1 **FAM19A3** PARD3B **ALMS1P**
10 HERC2
11 SLC26A7
12 NRSN1
13 EFCAB5 **TFAP2D**
14 NAV3
15 XKR4
16 BBOX1 **ALOX5** AL592494.3
17 C2orf34
18 TRPC4
19 THSD4
20 ARHGAP6 **ALMS1** RP11-615J4.4 **AC009499.1** MRPL33
21 **ARL15** ACCN1 **PDSS2** JAK1 **PDE4B** RP3-433F14.1
22 RP4-781K5.2
23 KIAA0146
24 COL5A3
25 PDE3B
26 MBD5
27 RP11-202P11.1

which are associated to common GO terms come together, other clusters which are over-represented in GO terms are being 'diluted' and the significance of the over-represented GO terms is being reduced.

The raw cluster data will be available upon request from alan.todd@pharmacy.ac.uk and in the future from a webpage.

DISCUSSION

Introns have often been assumed to be mutationally neutral. However, there is growing interest in blocks of intronic regions which are conserved across species and which have been suggested as candidate areas of *trans*-acting regulatory regions (54–56). Although we have only examined a single species in the present analysis, the same reasoning can be applied to paraloguous regions as well as orthologues. Indeed, genes which are

Table 8. Number of clusters whose associated GO terms were found to be over-represented using FuncAssociate

Cycle number	Clusters with over-represented GO terms	Sum of GO terms over-represented in each cluster	Number of clusters occurring in >10 different genes	% Clusters with over represented GO terms
5	16	94	133	12.030075188
9	22	120	219	10.0456621005
13	33	201	389	8.48329048843
17	65	291	642	10.1246105919
20	94	367	1048	8.96946564885
23	169	532	1768	9.55882352941
26	268	772	2921	9.17494008901
29	348	862	3620	9.61325966851
32	311	670	3167	9.82001894537
36	196	392	1824	10.7456140351
39	111	240	1060	10.4716981132
42	86	230	506	16.9960474308
45	54	207	238	22.6890756303
48	50	331	100	50.0

co-expressed and have a common regulatory mechanism do not necessarily have to be paralogues; the same *cis*-acting promoter binding motifs, for example, often exist upstream of unrelated genes. From a sequence conservation point of view, it is perhaps more remarkable to find large numbers of similar sequences in unrelated genes as in closely related ones. One could argue that it is possible for similar sequences in closely related genes to be simply passenger sequences which have not yet had time to diverge. In less closely related genes, it could even be argued that mutational cold spots (57) are responsible for some of the conserved sequence. Since we have identified clusters in genes whose members have a range of genetic distances from the closely related zinc finger genes in Figure 5 to the unrelated genes in Figure 9, we feel confident in stating that selective pressure is likely to be responsible for many of the sequence clusters observed here. The range of types of cluster and sequence types suggests that they have many different biological roles.

Eddy and Maizels (4) showed that there was a relationship between gene function and the number of PQ sequences found within those genes. By finding clusters which are over-represented in particular GO terms, we have shown that this type of relationship also applies at the sequence level and we can use the clusters to examine it further.

By comparing the sequences in a multiple sequence alignment, we may see which elements are conserved and which are variable. If the sequence group forms a quadruplex structure then some of these conserved and variable regions may not be critical in quadruplex formation but may be critical bases for molecular recognition. In certain cases, this would be more useful than simply finding quadruplex-dependent positions.

Whether one takes the abundance of similar PQs as evidence of selective pressure or not, the clustering data may still be exploited. For example, one of the key areas

of G-quadruplex research currently focuses on developing ligands which block transcription by stabilizing a particular quadruplex sequence. It may be important to know how unique that sequence is in order to provide specificity.

Meaningfulness of clusters

Since the clusters were merged using the full-linkage method, then the similarity threshold will be the lowest score between any pair of sequences in a cluster. At Cycle 16 (where most of the examples are from), the similarity threshold was 0.8. For a comparison of sequences where the shortest sequence is around 24 bases long, similar to the majority of cases in the cluster in Figure 4, the worst alignments would have to contain, for example three mismatches and two gaps which would give a similarity score of 0.808. In practice, the majority of alignments in that cluster are much more similar and this generally appears to be the case.

We have derived clusters of varying similarity and size, which raises the question of what represents a biologically relevant cluster. As the clustering progresses, less similar sequences are added to each cluster and at some stage the members will be merged, which do not have a similar biological role. The point at which this occurs is impossible to determine without knowledge of the role of these sequences or without experimental evidence. In the cases where we have discretely grouped clusters, rather than continuous merging through the clustering process, this should be less of a problem. We suggest that sequence types whose significance is determined in the future may have differing roles and so will require different degrees of similarity. Indeed, the cluster examples which we have presented were chosen because they represent a variety of different types of correlation: clusters which had a correlation with gene ontologies, those which correlated with protein families, clusters which belonged to disparate protein families and an example of a cluster which was found because of a particular interest (TERRA). The TERRA cluster is also an example which contains sequences that are known to form stable DNA and RNA quadruplexes.

The clustering in this study was performed on introns of human genes. It is now possible to examine other regions of genomic DNA with this methodology and search for clusters in, for example UTR regions, promoter regions or exons. The sequences which were clustered here are those which we selected using our criteria of four runs of at least three guanines, separated by loop regions. However, guanine quadruplex structures may not necessarily be formed exclusively from this sequence type. Indeed, in light of a recent structural study by Kuryavyi and Patel (58), we feel that a clustering approach using a yet more general rule for which sequences can potentially form quadruplex structures, will in due course bear fruit. This structure is not the only one to report a G-quadruplex with a topology which involves more than a simple sequence containing G-tracts separated by loop sequences; see in particular the molecular structures of the sequence in the promoter region of the *c-kit* gene (22–25). Clustering methods can be applied to any group of

sequences including, for example those which follow a specific template and those which are generally G-rich.

SUPPLEMENTARY DATA

Supplementary Data are available at NAR Online.

FUNDING

Conflict of interest statement. None declared.

REFERENCES

1. Todd,A.K., Johnston,M. and Neidle,S. (2005) Highly prevalent putative quadruplex sequence motifs in human DNA. *Nucleic Acids Res.*, **33**, 2901–2907.
2. D'Antonio,L. and Bagga,P. (2004) Computational methods for predicting intramolecular G-quadruplexes in nucleotide sequences. 3rd International IEEE Computer Society Computational Systems Bioinformatics Conference (CSB 2004). *IEEE Computer Society*, pp. 590–591.
3. Huppert,J.L. and Balasubramanian,S. (2005) Prevalence of quadruplexes in the human genome. *Nucleic Acids Res.*, **33**, 2908–2916.
4. Eddy,J. and Maizels,N. (2006) Gene function correlates with potential for G4 DNA formation in the human genome. *Nucleic Acids Res.*, **34**, 3887–3896.
5. Todd,A.K. and Neidle,S. (2008) The relationship of potential G-quadruplex sequences in *cis*-upstream regions of the human genome to SP1-binding elements. *Nucleic Acids Res.*, **36**, 2700–2704.
6. Eddy,J. and Maizels,N. (2009) Selection for the G4 DNA motif at the 5' end of human genes. *Mol. Carcinogenesis*, **48**, 319–325.
7. Huppert,J.L. and Balasubramanian,S. (2007) G-quadruplexes in promoters throughout the human genome. *Nucleic Acids Res.*, **35**, 406–413.
8. Hershman,S.G., Chen,Q., Lee,J.Y., Kozak,M.L., Yue,P., Wang,L.-S. and Johnson,F.B. (2008) Genomic distribution and functional analyses of potential G-quadruplex-forming sequences in Saccharomyces cerevisiae. *Nucleic Acids Res.*, **36**, 144–156.
9. Rawal,P., Kummarasetti,V.B.R., Ravindran,J., Kurmar,N., Halder,K., Sharma,R., Mukerji,M., Das,S.K. and Chowdhury,S. (2006) Genome-wide prediction of G4 DNA as regulatory motifs: role in *Escherichia coli* global regulation. *Genome Res.*, **16**, 644–655.
10. Eddy,J. and Maizels,N. (2008) Conserved elements with potential to form polymorphic G-quadruplex structures in the first intron of human genes. *Nucleic Acids Res.*, **36**, 1321–1330.
11. Todd,A.K., Haider,S.M., Parkinson,G.N. and Neidle,S. (2007) Sequence occurrence and structural uniqueness of a G-quadruplex in the human c-kit promoter. *Nucleic Acids Res.*, **35**, 5799–5808.
12. Huppert,J.L., Bugaut,A., Kumari,S. and Balasubramanian,S. (2008) G-quadruplexes: the beginning and end of UTRs. *Nucleic Acids Res.*, **36**, 6260–6268.
13. Du,Z., Kong,P., Gao,Y. and Li,N. (2007) Enrichment of G4 DNA motif in transcriptional regulatory region of chicken genome. *Biochem. Biophys. Res. Commun.*, **354**, 1067–1070.
14. Zhao,Y., Du,Z. and Li,N. (2007) Extensive selection for the enrichment of G4 DNA motifs in transcriptional regulatory regions of warm blooded animals. *FEBS Lett.*, **581**, 1951–1956.
15. Todd,A.K. (2007) Bioinformatics approaches to quadruplex sequence location. *Methods*, **43**, 246–251.
16. Huppert,J.L. (2006) Quadruplexes in the genome. In Neidle,S. and Balasubramanian,S. (eds), *Quadruplex Nucleic Acids*. Royal Society of Chemistry, Cambridge, pp. 208–227.
17. Zhang,R., Lin,Y. and Zhang,C.-T. (2007) Greglist: a database listing potential G-quadruplex regulated genes. *Nucleic Acids Res.*, **36**, D372–D376.
18. Kostadinov,R., Malhotra,N., Viotti,M., Shine,R., D'Antonio,L. and Bagga,P. (2006) GRSDB: a database of quadruplex forming G-rich sequences in alternatively processed mammalian pre-mRNA sequences. *Nucleic Acids Res.*, **34**, D119–D124.
19. Yadav,V.K., Abraham,J.K., Mani,P., Kulshrestha,R. and Chowdhury,S. (2008) QuadBase: genome-wide database of G4 DNA occurrence and conservation in human, chimpanzee, mouse and rat promoters and 146 microbes. *Nucleic Acids Res*, **36**, D381–D385.
20. Kikin,O., Zappala,Z., D'Antonio,L. and Bagga,P.S. (2008) GRSDB2 and GRS_UTRdb: databases of quadruplex forming G-rich sequences in pre-mRNAs and mRNAs. *Nucleic Acids Res.*, **39**, D141–D148.
21. Kikin,O., D'Antonio,L. and Bagga,P. (2006) QGRS Mapper: a web-based server for predicting G-quadruplexes in nucleotide sequences. *Nucleic Acids Res.*, **34**, W676–W682.
22. Rankin,S., Reszka,A.P., Huppert,J., Zloh,M., Parkinson,G.N., Todd,A.K., Ladame,S., Balasubramanian,S. and Neidle,S. (2005) Putative DNA quadruplex formation within the human c-kit oncogene. *J. Am. Chem. Soc.*, **127**, 10584–10589.
23. Phan,A.T., Kuryavyi,V., Burge,S., Neidle,S. and Patel,D.J. (2007) Structure of an unprecedented G-quadruplex scaffold in the human c-kit promoter. *J. Am. Chem. Soc.*, **129**, 4386–4392.
24. Fernando,H., Reszka,A.P., Huppert,J.L., Ladame,S., Rankin,S., Venkitaraman,A.R., Neidle,S. and Balasubramanian,S. (2006) A conserved quadruplex motif located in a transcription activation site of the human c-kit oncogene. *Biochemistry*, **45**, 7854–7860.
25. Hsu,S.T., Varnai,P., Bugaut,A., Reszka,A.P., Neidle,S. and Balasubramanian,S. (2009) A G-rich sequence within the c-kit oncogene promoter forms a parallel G-quadruplex having asymmetric G-tetrad dynamics. *J. Am. Chem. Soc.*, **131**, 13399–13409.
26. Phan,A.T., Modi,Y.S. and Patel,D.J. (2004) Propeller-type parallel-stranded G-quadruplexes in the human c-myc promoter. *J. Am. Chem. Soc.*, **126**, 8710–8716.
27. Ambrus,A., Chen,D., Dai,J., Jones,R.A. and Yang,D. (2005) Solution structure of the biologically relevant G-quadruplex element in the human c-MYC promoter. Implications for G-quadruplex stabilization. *Biochemistry*, **44**, 2048–2058.
28. Kumari,S., Bugaut,A., Huppert,J.L. and Balasubramanian,S. (2007) An RNA G-quadruplex in the 5' UTR of the NRAS proto-oncogene modulates translation. *Nature Chem. Biol.*, **3**, 218–221.
29. Arora,A., Dutkiewicz,M., Scaria,V., Hariharan,M., Maiti,S. and Kurreck,J. (2008) Inhibition of translation in living eukaryotic cells by an RNA G-quadruplex motif. *RNA*, **14**, 1290–1296.
30. Wang,Y. and Patel,D.J. (1993) Solution structure of the human telomeric repeat D[Ag$_3$(T$_2$Ag$_3$)$_3$] G-tetraplex. *Structure*, **1**, 263–282.
31. Parkinson,G.N., Lee,M.P. and Neidle,S. (2002) Crystal structure of parallel quadruplexes from human telomeric DNA. *Nature*, **417**, 876–880.
32. Ambrus,A., Chen,D., Dai,J., Bialis,T., Jones,R.A. and Yang,D. (2006) Human telomeric sequence forms a hybrid-type intramolecular G-quadruplex structure with mixed parallel/antiparallel strands in potassium solution. *Nucleic Acids Res.*, **34**, 2723–2735.
33. Lim,K.W., Amrane,S., Bouaziz,S., Xu,W., Mu,Y., Patel,D.J., Luu,K.N. and Phan,A.T. (2009) Structure of the human telomere in K+ solution: a stable basket-type G-quadruplex with only two G-tetrad layers. *J. Am. Chem. Soc.*, **131**, 4301–4309.
34. Risitano,A. and Fox,K.R. (2004) Influence of loop size on the stability of intramolecular DNA quadruplexes. *Nucleic Acids Res.*, **32**, 2598–2606.
35. Bugaut,A. and Balasubramanian,S. (2008) A sequence-independent study of the influence of short loop lengths on the stability and topology of intramolecular DNA G-quadruplexes. *Biochemistry*, **47**, 689–697.
36. Guédin,A., Alberti,P. and Mergny,J.-L. (2009) Stability of intramolecular quadruplexes: sequence effects in the central loop. *Nucleic Acids Res.*, **37**, 5559–5567.

37. Rachwal,P.A., Brown,T. and Fox,K.R. (2007) Sequence effects of single base loops in intramolecular quadruplex DNA. *FEBS Lett.*, **581**, 1657–1660.

38. Stegle,O., Payet,L., Mergny,J.L., MacKay,D.J. and Huppert,J.L. (2009) Predicting and understanding the stability of G-quadruplexes. *Bioinformatics*, **25**, i374–i382.

39. Johnson,S.C. (1967) Hierarchical clustering schemes. *Psychometrica*, **32**, 241–254.

40. Hubbard,T.J.P., Aken,B.L., Ayling,S., Ballester,B., Beal,K., Bragin,E., Brent,S., Chen,Y., Clapham,P., Clarke,L. *et al.* (2009) Ensembl 2009. *Nucleic Acids Res.*, **37**, D690–D697.

41. Durbin,R., Eddy,S.R., Krogh,A. and Mitchison,G. (2002) *Biological Sequence Analysis. Probabilistic Models of Proteins and Nucleic Acids*. Cambridge University Press, UK.

42. Larkin,M.A., Blackshields,G., Brown,N.P., Chenna,R., McGettigan,P.A., McWilliam,H., Valentin,F., Wallace,I.M., Wilm,A., Lopez,R. *et al.* (2007) Clustal W and Clustal X version 2.0. *Bioinformatics*, **23**, 2947–2948.

43. Berriz,G.F., Beaver,J.E., Cenik,C., Tasan,M. and Roth,F.P. (2009) Next generation software for functional trend analysis. *Bioinformatics*, **25**, 3043–3044.

44. The Gene Ontology Consortium. (2000) Gene ontology: tool for the unification of biology. *Nat. Genet.*, **25**, 25–9.

45. Azzalin,C.M., Reichenbach,P., Khoriauli,L., Giulotto,E. and Lingner,J. (2007) Telomeric repeat containing RNA and RNA surveillance factors at mammalian chromosome ends. *Science*, **318**, 798–801.

46. Schoeftner,S. and Blasco,M.A. (2008) Developmentally regulated transcription of mammalian telomeres by DNA-dependent RNA polymerase II. *Nat. Cell Biol.*, **10**, 228–236.

47. Randall,A. and Griffith,J.D. (2009) Structure of long telomeric RNA transcripts. *J. Biol. Chem.*, **284**, 13980–13986.

48. Meyne,J., Baker,R.J., Hobart,H.H., Hsu,T.C., Ryder,O.A., Ward,O.G., Wiley,J.E., Wurster-Hill,D.H., Yates,T.L. and Moyzis,R.K. (1990) Distribution of non-telomeric sites of the (TTAGGG)n telomeric sequence in vertebrate chromosomes. *Chromosoma*, **99**, 3–10.

49. Mulder,N.J., Apweiler,R., Attwood,T.K., Bairoch,A., Bateman,A., Binns,D., Bork,P., Buillard,V., Cerutti,L., Copley,R. *et al.* (2007) New developments in the InterPro database. *Nucleic Acids Res.*, **35**, D224–D228.

50. Kuoa,T.-Y., Hongb,C.-J. and Yi-Ping Hsueh,Y.-P. (2009) Bcl11A/ CTIP1 regulates expression of DCC and MAP1b in control of axon branching and dendrite outgrowth. *Mol. Cell. Neurosci.*, **42**, 195–207.

51. Balakirev,E.S. and Ayala,F.J. (2003) Pseudogenes: are they "junk" or functional DNA? *Annu. Rev. Genet.*, **37**, 123–151.

52. Poliseno,L., Salmena,L., Zhang,J., Carver,B., Haveman,W.J. and Pandolfi,P.P. (2010) A coding-independent function of gene and pseudogene mRNAs regulates tumour biology. *Nature*, **465**, 1033–1038.

53. Haider,S., Ballester,B., Smedley,D., Zhang,J., Rice,P. and Kasprzyk,A. (2009) BioMart Central Portal - unified access to biological data. *Nucleic Acids Res.*, **37**, W23–W27.

54. Hare,M.P. and Palumbi,S.R. (2003) High intron sequence conservation across three mammalian orders suggests functional constraints. *Mol. Biol. Evol.*, **20**, 969–978.

55. Wasserman,W.W., Palumbo,M., Thompson,W., Fickett,J.W. and Lawrence,C.E. (2000) Human–mouse genome comparisons to locate regulatory sites. *Nat. Genet.*, **26**, 225–228.

56. Dermitzakis,E.T., Reymond,A., Lyle,R., Scamuffa,N., Ucla,C., Deutsch,S., Stevenson,B.J., Flegel,V., Bucher,P., Jongeneel,C.V. *et al.* (2002) Numerous potentially functional but non-genic conserved sequences on human chromosome 21. *Nature*, **420**, 578–582.

57. Clark,A.G. (2001) The search for meaning in noncoding DNA. *Genome Res.*, **11**, 1319–1320.

58. Kuryavyi,V. and Patel,D.J. (2010) Solution structure of a unique G-quadruplex scaffold adopted by a guanosine-rich human intronic sequence. *Structure*, **18**, 73–82.